Angewandte Chemie
Eine Zeitschrift der Gesellschaft Deutscher Chemiker

Supporting Information

A Metal–Organic Framework derived $Cu_xO_yC_z$ Catalyst for Electrochemical CO_2 Reduction and Impact of Local pH Change

*Nivedita Sikdar[+], João R. C. Junqueira[+], Stefan Dieckhöfer, Thomas Quast, Michael Braun, Yanfang Song, Harshitha B. Aiyappa, Sabine Seisel, Jonas Weidner, Denis Öhl, Corina Andronescu, and Wolfgang Schuhmann**

anie_202108313_sm_miscellaneous_information.pdf

Supporting Information

Experimental section

Chemicals and materials:

The chemicals were used as received, except noted otherwise. Copper nitrate salt [$Cu(NO_3)_2 \cdot 2.5H_2O$] and 1,3,5-benzenetricarboxylic acid (H_3BTC) were purchased from Alfa Aesar. Ethanol (absolute) was purchased from VWR Chemicals and potassium hydroxide (KOH) was from Fisher Scientific. Poly(tetrafluoroethylene) (PTFE) (1 μm particle size) was purchased from Sigma Aldrich. Gas diffusion electrodes (GDE) were from Freudenberg (H23C2). Carbon dioxide (CO_2), argon (Ar), nitrogen (N_2) and oxygen (O_2) gas bottles were from Air Liquide. All aqueous solutions were prepared by using deionized water from a Millipore purification system (resistivity =18.2 MΩ) and KOH was purified before using with a Chelex® resin column.

Characterizations:

X-ray diffraction (XRD) data were obtained using a Bruker D8 Discover X-ray diffractometer equipped with a Cu Kα radiation source (λ = 1.5418 Å). For data treatment and evaluation, the Bruker software DIFFRAC.EVA has been used. Scanning electron micrographs were recorded using a Quanta 3D ESEM (FEI) operated at 30.0, 20.0, 10.0 and 5.0 kV for SEM imaging and elemental mapping in the high vacuum mode. Transmission electron microscopy (TEM) and high resolution TEM (HRTEM) was performed with a JEOL microscope (JEM-2800) equipped with Schottky-type emission source working at 200 kV, Gatan OneView camera (4kx4k, 25FPS) to obtain images with a resolution of 0.09 nm. Energy dispersive spectroscopy elemental mapping was performed using double silicon drift detectors, with a solid angle of 0.98 steradians with a detection area of 100 mm^2. X-ray photoelectron spectroscopy (XPS) measurements were carried using two setups: the AXIS Nova spectrometer equipped with a monochromatic Al Kα X-ray source (1487 eV, 15 mA emission current) and ULVAC-PHI VersaProbe II equipped with a monochromatic Al Kα X-ray source (1486.6 eV) with dual-beam charge neutralization. Throughout all measurements, the instrument maintained pressure around 10^{-8} Torr within the sample analysis chamber. A low-energy electron flood gun was applied for charge neutralization. Calibration of the binding

energy scale was conducted by assigning the C 1s peak of carbon to a value of 284.8 eV. For XPS deconvolution, reference spectra of Cu, Cu_2O, CuO, $Cu(OH)_2$ or $CuCO_3$ reported in the literature were used. For example, for the CuO, 5 peaks with defined FWHM and defined relative positions to each other were added during the fitting process. The fitting process was automatically conducted using the software CasaXPS or ESCApe. In general, deconvolution of all samples showed the presence of Cu, Cu_2O, and CuO species. In the deconvoluted graphs, we labeled just the species whose total peak contribution is higher than the detection limit of XPS, ± 3 at%. For example, in the sample HKUST@800, a small contribution of Cu^0 and $Cu(OH)_2$ can be observed, marked with purple and dark green colour. Still, the total amount of these species on the catalyst surface results to be ~ 1%. Being below the detection limit, we cannot, therefore, undoubtedly attribute this contribution to Cu^0 or $Cu(OH)_2$.

Synthesis of HKUST:

$Cu(NO_3)_2 \cdot 2.5H_2O$ (0.232 g, 1 mmol) and H_3BTC (0.170 g, 0.81 mmol) were dissolved in 12 mL of DMF/ethanol/water mixture (v/v = 1:1:1) in a 100 mL glass bottle. The whole solution is sonicated for 5 mins and the bottle was sealed properly. This is now placed in a preheated oven at 70 °C for 24 h. The dark blue colored crystals (HKUST) were taken out and cooled slowly to room temperature. The crystals were then washed with EtOH for three to four times followed by drying in ambient condition.

Synthesis of HKUST derived $Cu_xO_yC_z$ catalyst:

The above prepared HKUST crystals (~0.5 g) were placed in a tube furnace for carbonization, which was conducted at 400 °C, 600 °C, 800 °C and 1000 °C for 4 h under O_2/Ar atmosphere (1:9 v/v). The heating rate to reach the desired temperature was set to 10 °C min^{-1}. The obtained catalyst powders were denoted as HKUST@400, HKUST@600, HKUST@800 and HKUST@1000, respectively.

Preparation of electrodes (GDEs):

The working electrodes are commercial GDEs comprising of a microporous carbon layer on top of carbon paper (diameter: 2.4 cm, effective working electrode diameter 1.7 cm). This was modified with catalysts with (or without) different PTFE loading amounts (0, 5, 10, 25, 50, 100 and 200 wt%) with respect to the catalyst mass by drop-casting. The catalyst loading is kept constant around ~1 mg/cm^2. ~5 mg of catalyst powders was suspended in different PTFE-containing EtOH solutions (1 mL), and ultrasonicated for 45 min, maintaining the temperature of the water bath always at or below room temperature (adjusted with ice cubes). The whole catalysts ink solutions were transferred on GDE slowly by drop casting cautiously.

Electrochemical experiments:

A custom-made three-compartment glass electrochemical cell was used. The cell is comprised of two compartments, which were separated by an anion exchange membrane (AEM, FAB-PK-75, fumatech). One compartment, the anodic chamber, for the counter electrode (Ni foam) and the other one, cathodic compartment, for the reference (double junction Ag|AgCl (3 M KCl)) and working electrode (GDE). The WE was constantly supplied with CO_2 from the backside through the gas feed chamber. Before the measurement, the anodic and cathodic compartments were filled with 14 and 15 mL of electrolyte, respectively. The electrolyte was 1 M KOH. Chronopotentiometry for 870 s was performed followed by a 30 s galvanostatic EIS measurement at six different currents. In the galvanostatic EIS, the applied current varied from -20 to -120 mA/cm^2 (-45.2 to -271 mA, consider a geometric surface area of 2.27 cm^2 for working electrode) and the intensity of the current excitation was always 10 % of the applied current, e.g. at -20 mA/cm^2 (-45.2 mA) of applied current, the excitation was -2 mA/cm^2 (-4.52 mA). A representative galvanostatic EIS is added below for better clarity of the experimental conditions.

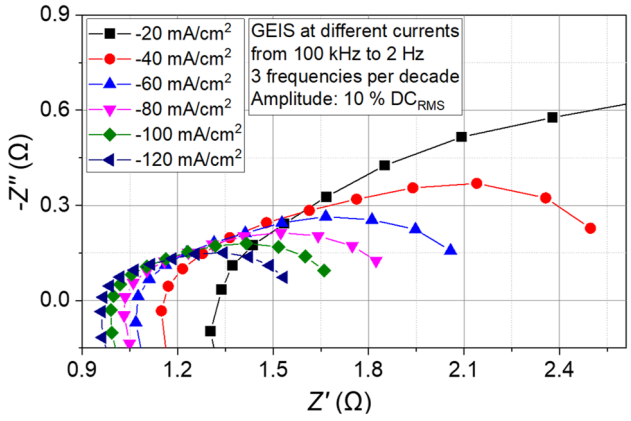

Figure: A representative galvanostatic EIS as recorded for 100 wt% PTFE loaded GDE.

During the measurement, two mass flow controllers (MFCs, AALBORG) were used to set a flow for N_2 (16 mL/min), to constantly purge the catholyte carrying the evolved bubbles to the GC and to exclude the presence of O_2, in the electrolyte, and for CO_2 (20 mL/min). Two ends of the reactor were connected to a 6-way valve, allowing to commute between the gaseous products evolved from the GDE (called *headspace* products) and the products in the CO_2 chamber (referred to as *gas feed compartment*) and at the same time maintaining a specific CO_2 back pressure.

The value of the applied potential values (vs. Ag/AgCl) was converted to the scale of the reversible hydrogen electrode (RHE) using the following equation, considering the electrolyte bulk pH of 1 M KOH solution equal to 13.9: $E_{\mathrm{RHE}} = E_{\mathrm{Ag|AgCl\ (3\ M\ KCl)}} + 0.210 + (0.059 * \mathrm{pH})$.

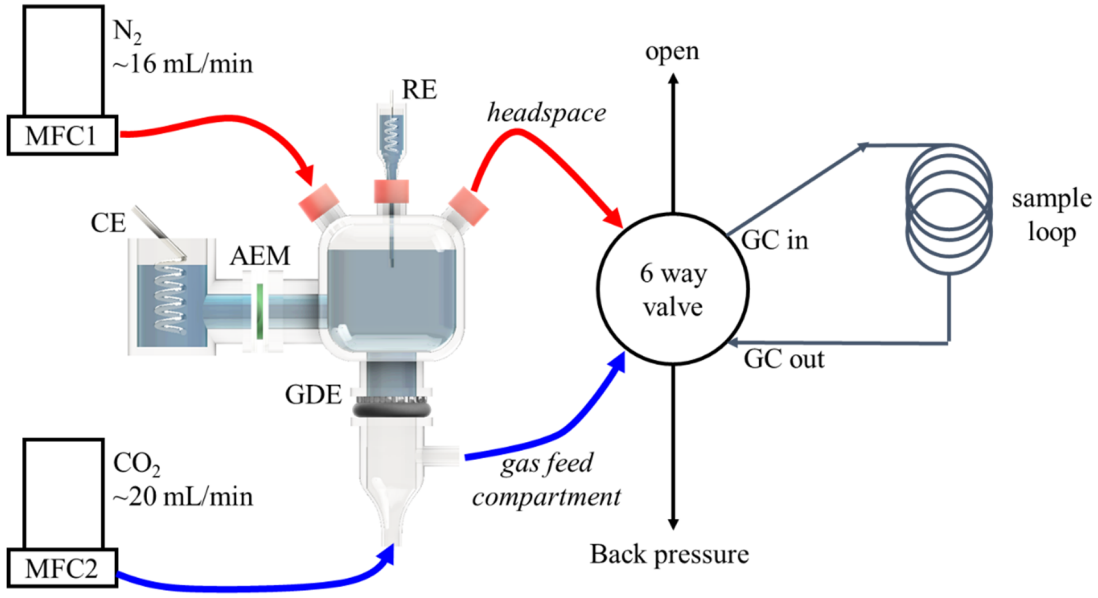

Scheme S1: Scheme of the on-line analysis of gaseous products using GC using the custom-made electrochemical reactor set up for CO_2RR analysis.

Products quantification:

Gas products were analyzed using a gas chromatography (GC multiple gas analyzer#1, SRI Instruments) with the sample loop (1 mL) connected to the reactor. H_2 was analyzed using thermal conductive detector (TCD) and CO, CH_4, C_2H_4, and C_2H_6 were analyzed using a flame ionization detector (FID) equipped with a methanizer. N_2 was the carrier gas (21 psi), the oven temperature was constant at 90 °C and a 3 meters HayeSep D was utilized as separating column. The GC parameters were tuned to separate all the products in 6 minutes and after each run, the sample loop was flushed with

new products for 1.5 minutes. Altogether, it was possible to inject new samples each 7.5 minutes. The same current was applied for 15 minutes allowing one injection of the *headspace* products (gaseous products that evolved from the GDE) and another for the *gas feed compartment* products (products in the CO_2 feed).

Liquid products: quantification using HPLC

HPLC was conducted with a Dionex ICS-5000 with Diode Array Detector at 220 nm and a Refractive Index Detector (RefractoMax520) detector. The column is an ion-exclusion column from Bio-Rad (Aminex HPX-87H) and the eluent is 4 mM sulfuric acid. We also used the corresponding guard column from Bio-Rad. 10 µL of sample was injected using an auto-sampler for each HPLC measurement. The sample analytes as collected (540 µL) during chronopotentiometry were neutralized with 2.5 M H_2SO_4 solution (sample:H_2SO_4 = 4:1, v/v) before submitting them to HPLC analysis.

Calculation of Faradaic Efficiency (%FE):

Formation rate of gaseous product:

$$\dot{n}_i = \frac{x_i \times f}{1{,}000{,}000 \times V_m} \text{ [mol/s]}$$

$\dot{n}_i$ = Formation rate of gaseous product in mol/s

x_i = Concentration of the product detected by GC in ppm

f = CO_2 gas flow rate in L/s

V_m = Molar volume of an ideal gas in 24.5 L/mol

Faraday law of electrolysis:

$$I_i = z_i n_i F, \text{ [A]}$$

I_i = Partial current for each product during CO_2 bulk electrolysis in A

z_i = Numbers of electrons transferred for each product

$\dot{n}_i$ = Formation rate of gaseous product in mol/s

F = Faraday constant 96485 in C/mol

Faradaic Efficiency:

$$FE_i = \left(\frac{I_i}{I_t}\right) \times 100 \text{ [\%]}$$

FE_i: Faradaic efficiency of the product in %

I_t: Total measured current during CO_2 bulk electrolysis in A

I_i = Partial current for each product during CO_2 bulk electrolysis in A

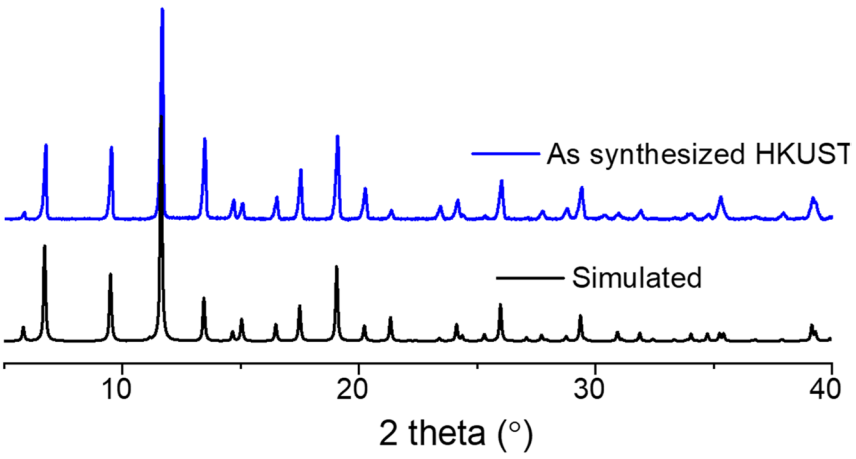

Figure S1: PXRD patterns of simulated and as synthesized HKUST MOF.

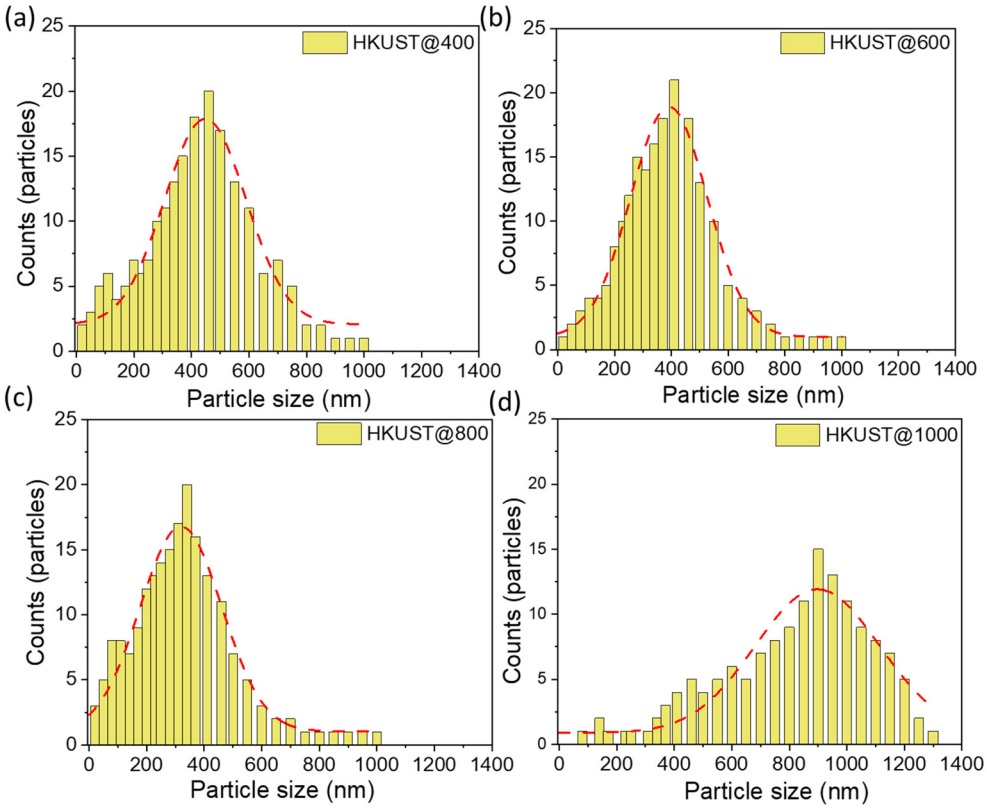

Figure S2: Average particle size distribution histograms of (a) HKUST@400 (b) HKUST@600 (c) HKUST@800 and (d) HKUST@1000.

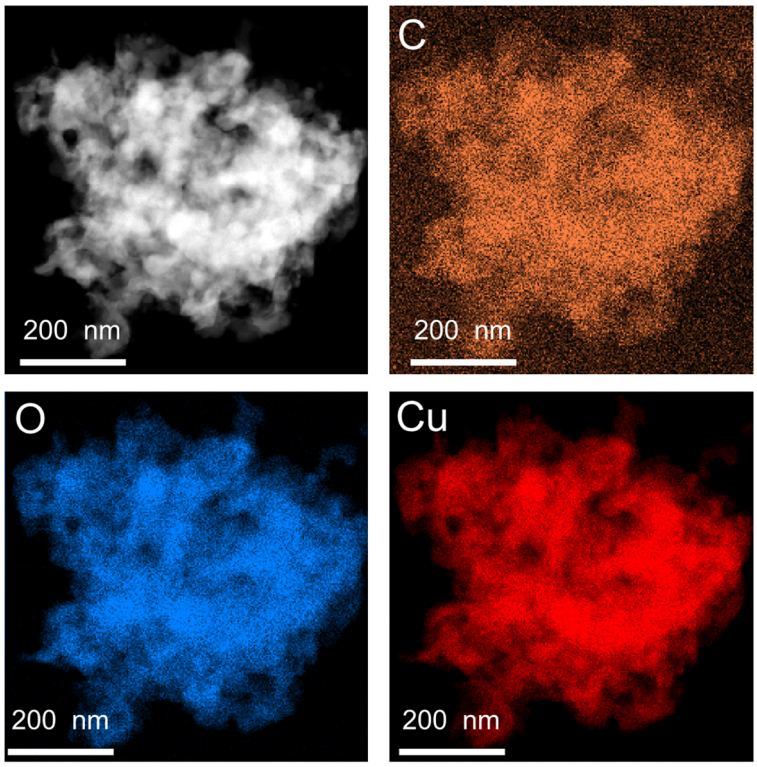

Figure S3: TEM-EDS elemental color map images of HKUST@400.

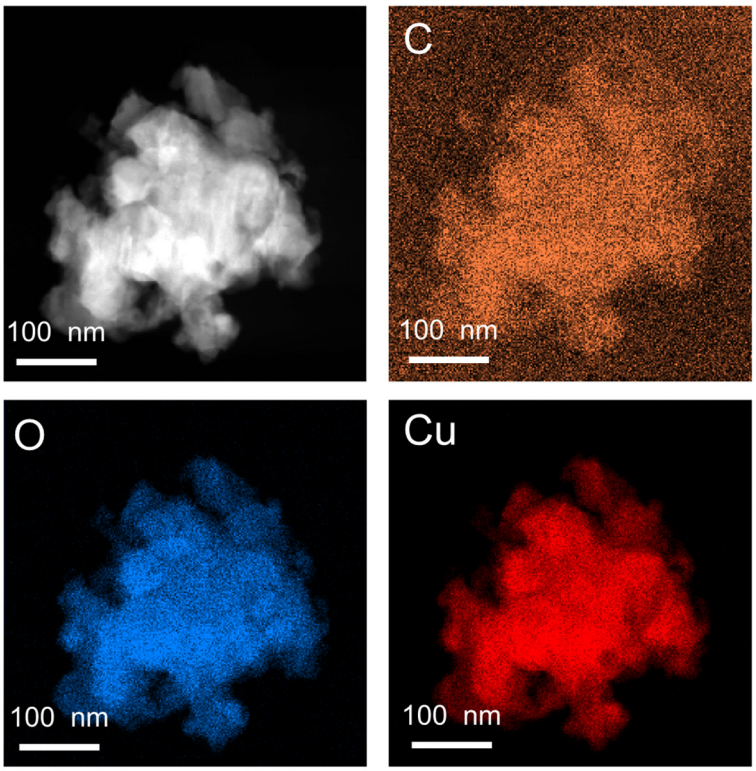

Figure S4: TEM-EDS elemental color map images of HKUST@600.

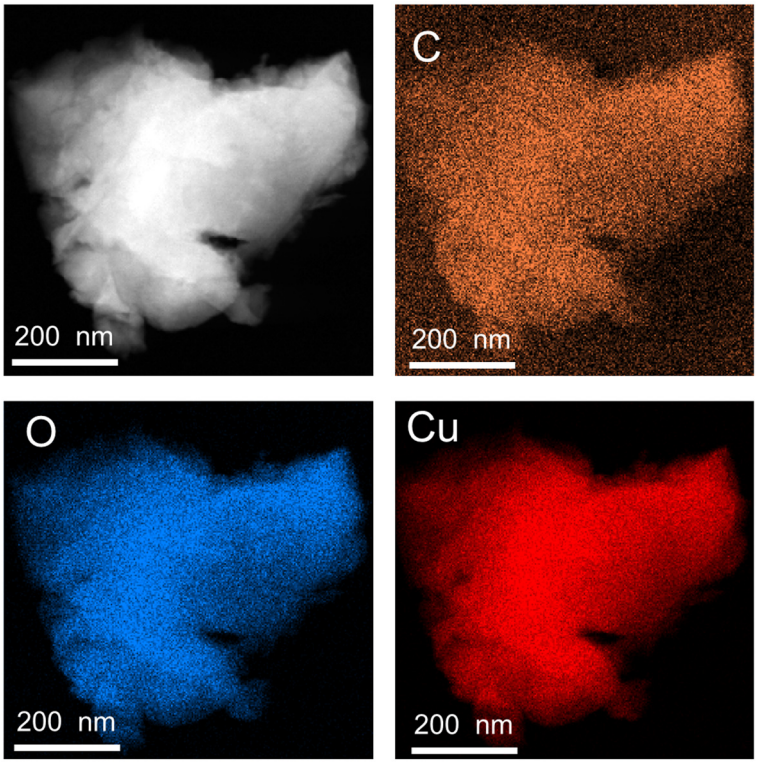

Figure S5: TEM-EDS elemental color map images of HKUST@1000.

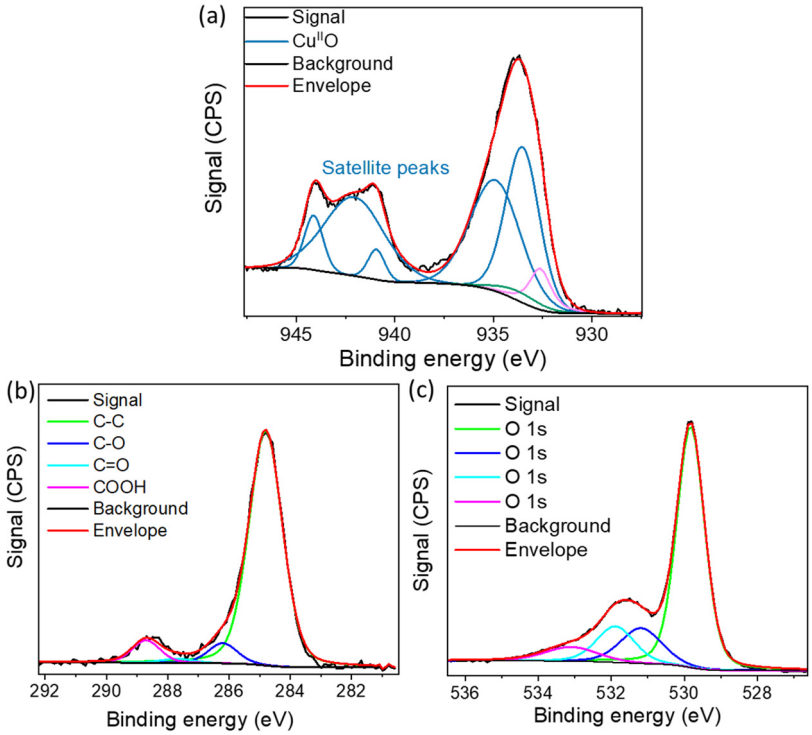

Figure S6: Deconvoluted XPS data of HKUST@400: (a) 2p3/2 core level peaks of Cu; (b) core level peaks of O 1s; and (c) core level peaks of C 1s.

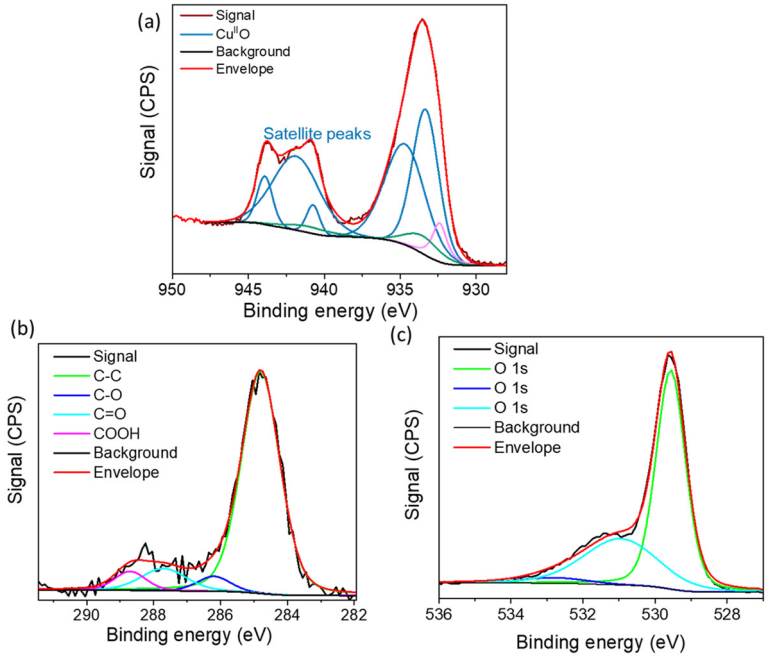

Figure S7: Deconvoluted XPS data of HKUST@600: (a) 2p3/2 core level peaks of Cu; (b) core level peaks of O 1s; and (c) core level peaks of C 1s.

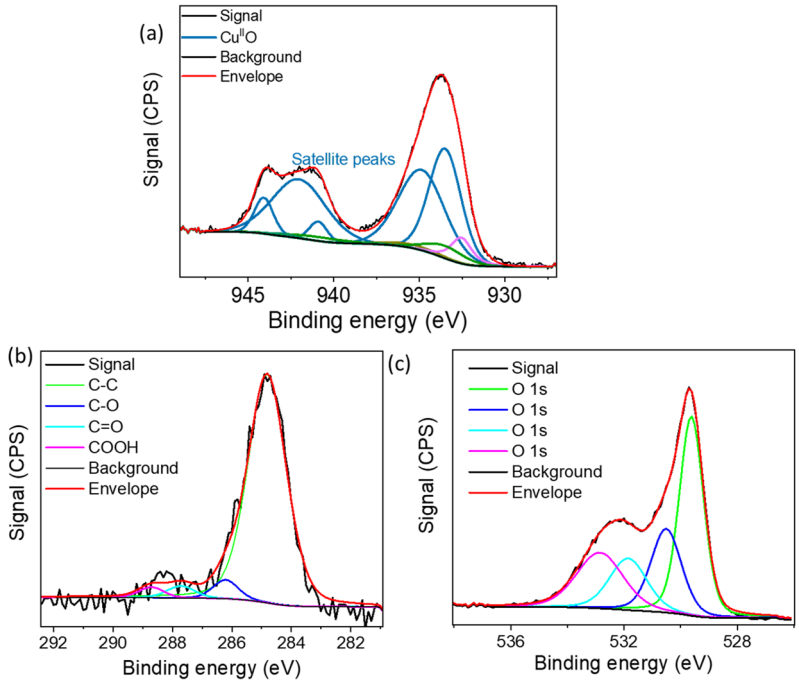

Figure S8: Deconvoluted XPS data of HKUST@800: (a) 2p3/2 core level peaks of Cu; (b) core level peaks of O 1s; and (c) core level peaks of C 1s.

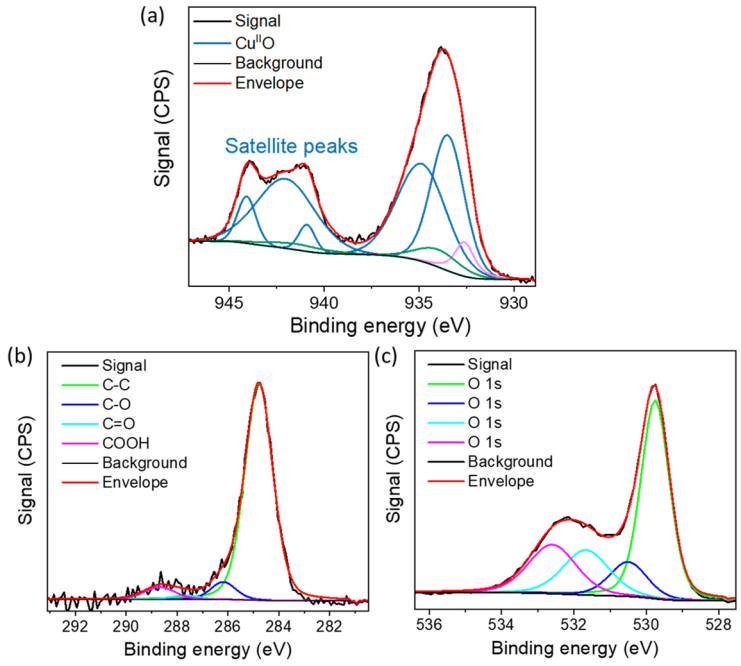

Figure S9: Deconvoluted XPS data of HKUST@1000: (a) 2p3/2 core level peaks of Cu; (b) core level peaks of O 1s; and (c) core level peaks of C 1s.

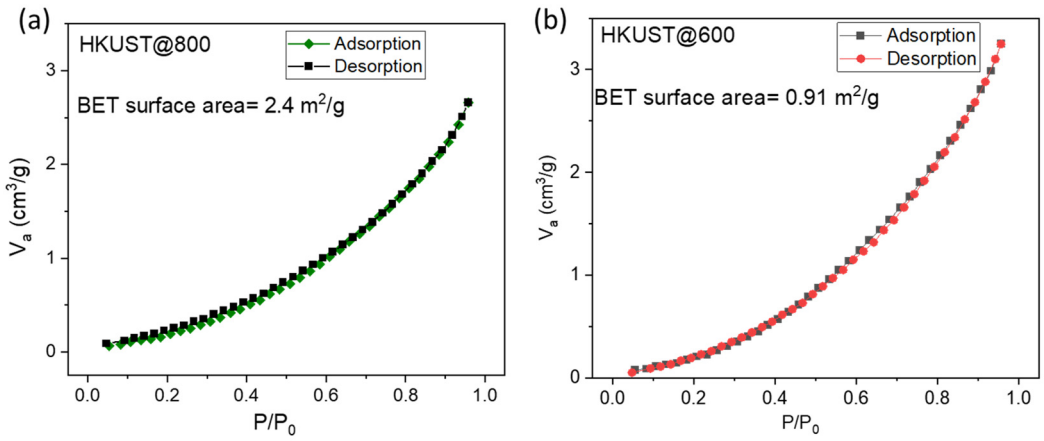

Figure S10: N_2 adsorption isotherms for HKUST@800 and HKUST@600 at 77 K.

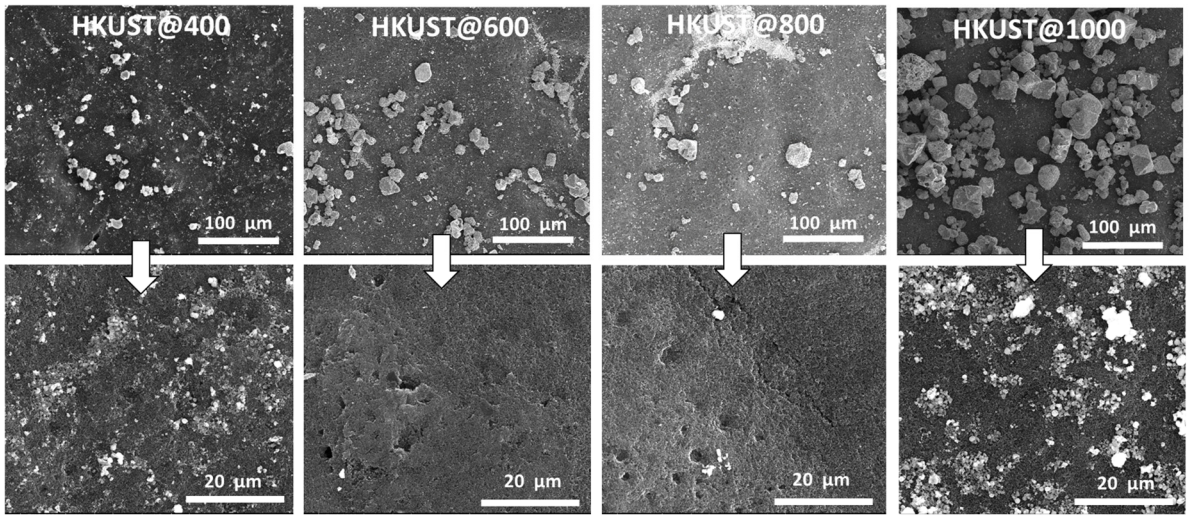

Figure S11: SEM images (at different magnification) of HKUST@400, HKUST@600, HKUST@800 and HKUST@1000 without PTFE support on GDEs.

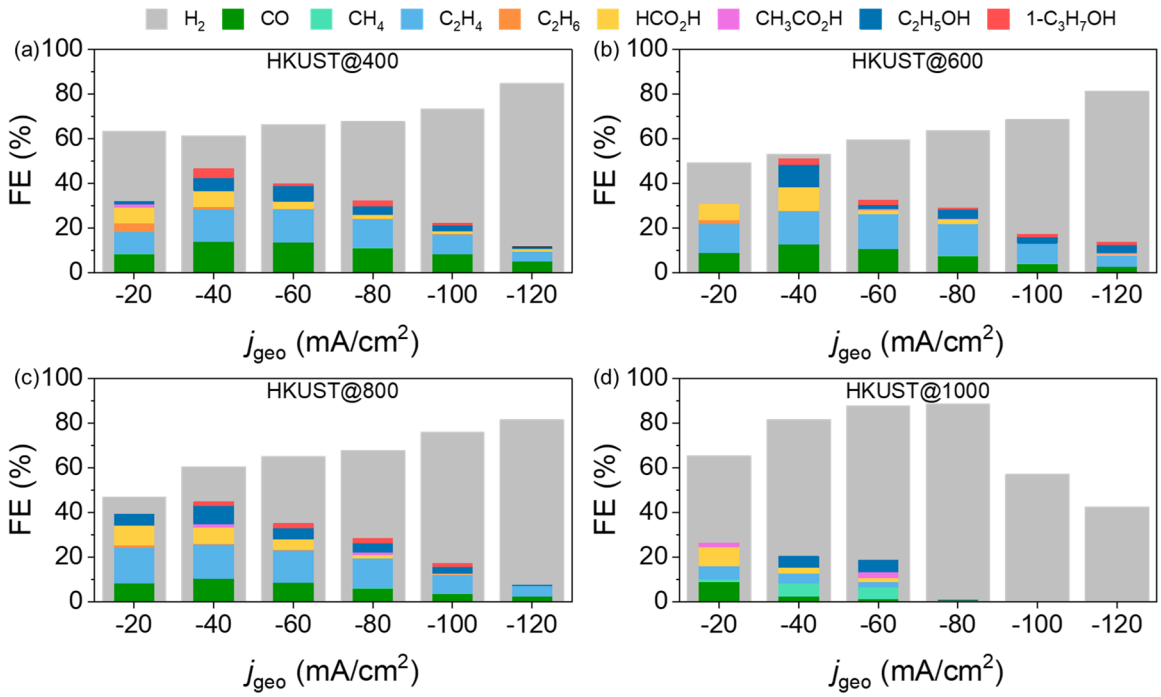

Figure S12: FE (%) for all products obtained from GDEs with HKUST-derived catalysts without PTFE (0 wt% PTFE) modification in dependence of the applied current density.

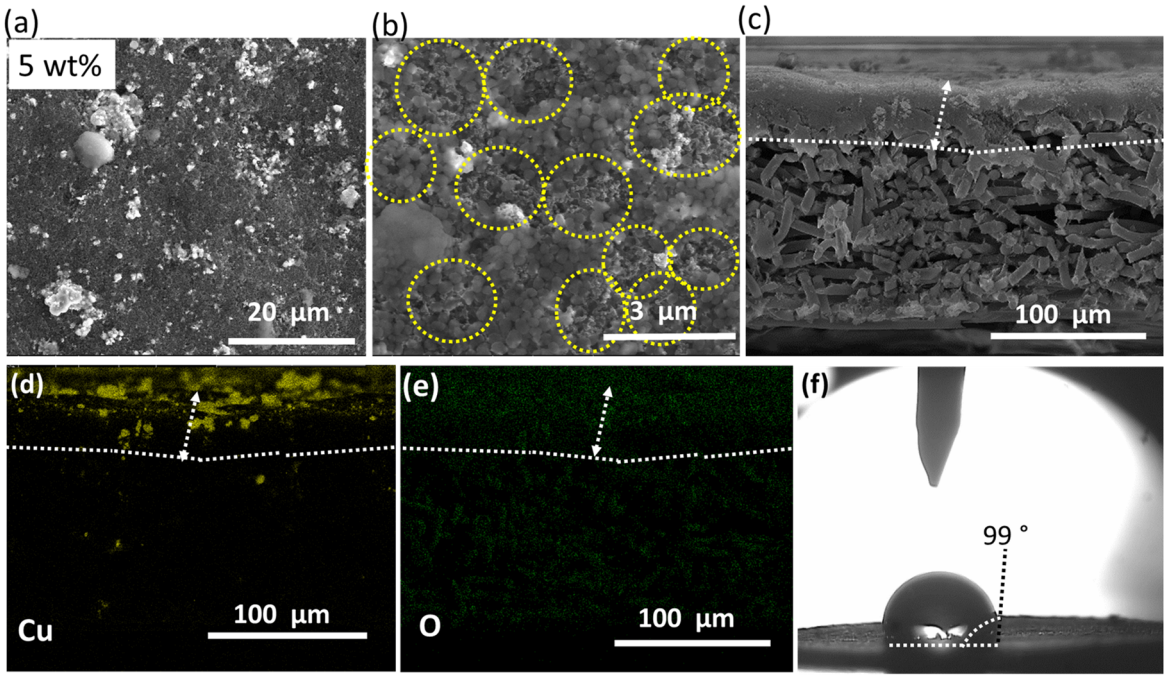

Figure S13: HKUST@800: (a-b) SEM images of 5 wt% PTFE supported GDE, captured at different magnifications. The round yellow circles in (b) represent PTFE/catalyst heterojunctions; (c) cross section view of GDE; (d-e) SEM-EDS elemental color maps along the cross-section showing distributions of Cu and O; (f) contact angle value of the same GDE.

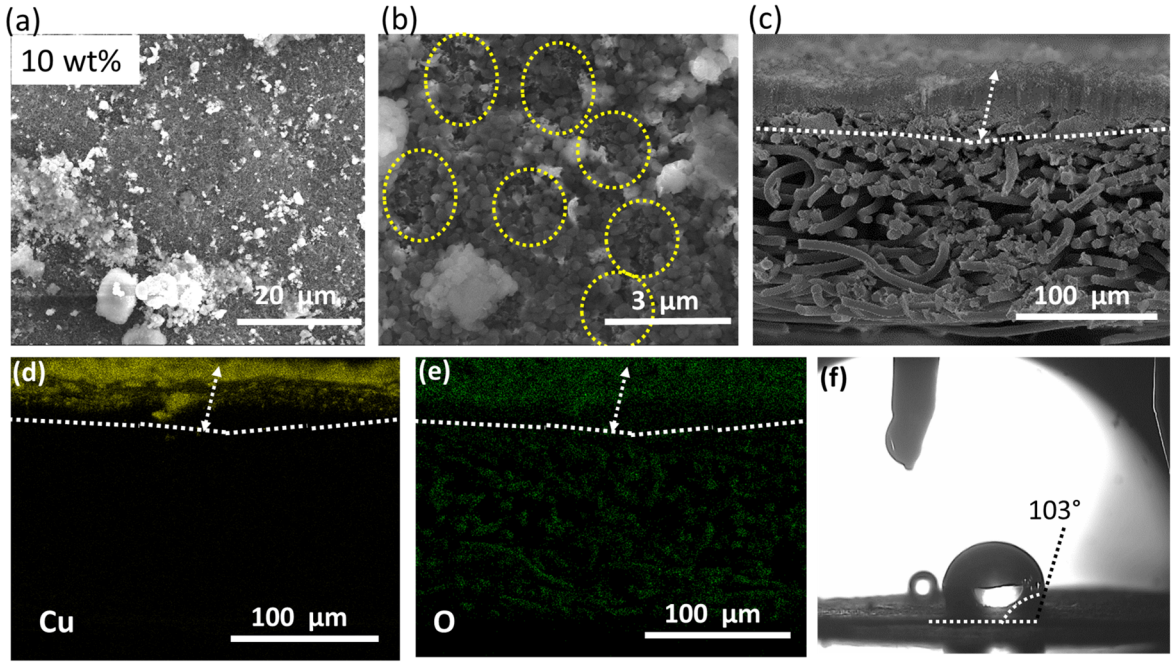

Figure S14: HKUST@800: (a-b) SEM images of 10 wt% PTFE supported GDE, captured at different magnifications. The round yellow circles in (b) represent PTFE/catalyst heterojunctions; (c) cross section view of GDE; (d-e) SEM-EDS elemental color maps along the cross-section showing distributions of Cu and O; (f) contact angle value of the same GDE.

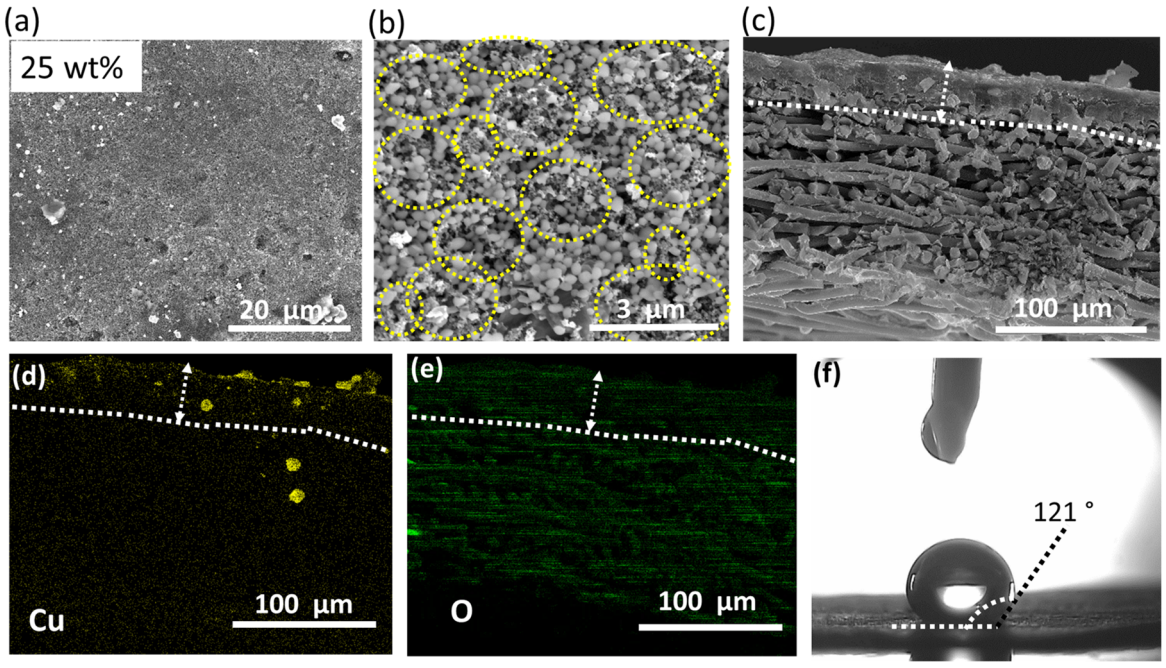

Figure S15: HKUST@800: (a-b) SEM images of 25 wt% PTFE supported GDE, captured at different magnifications. The round yellow circles in (b) represent PTFE/catalyst heterojunctions; (c) cross section view of GDE; (d-e) SEM-EDS elemental color maps along the cross-section showing distributions of Cu and O; (f) contact angle value of the same GDE.

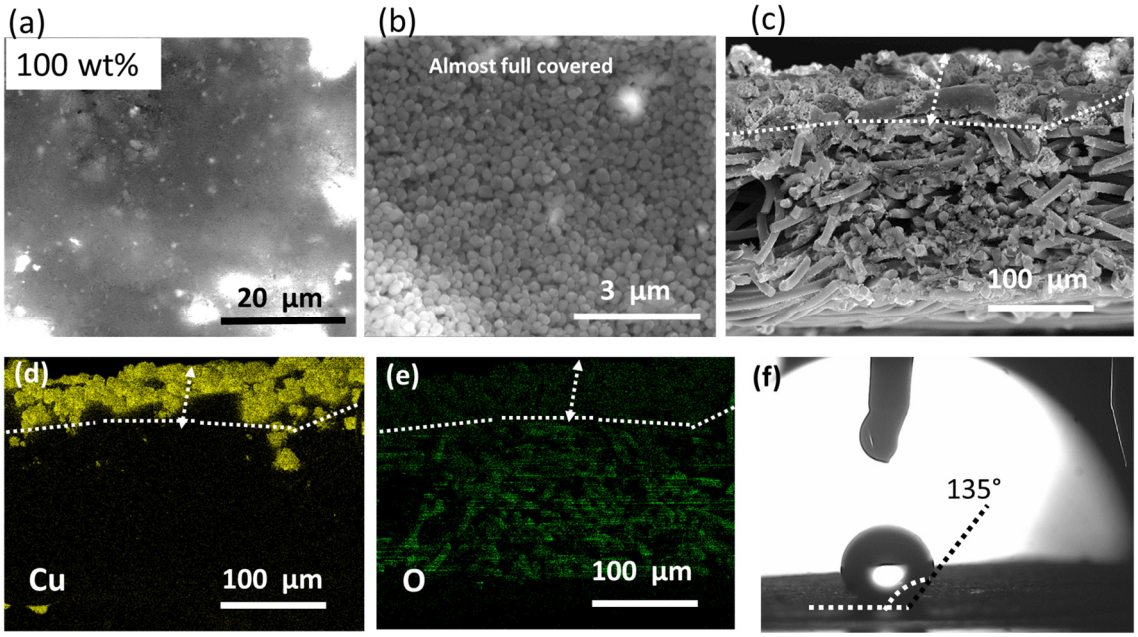

Figure S16: HKUST@800: (a-b) SEM images of 100 wt% PTFE supported GDE, captured at different magnifications; (c) cross section view of the GDE; (d-e) SEM-EDS elemental color maps along the cross section showing the distributions of Cu and O; (f) contact angle value of the same GDE.

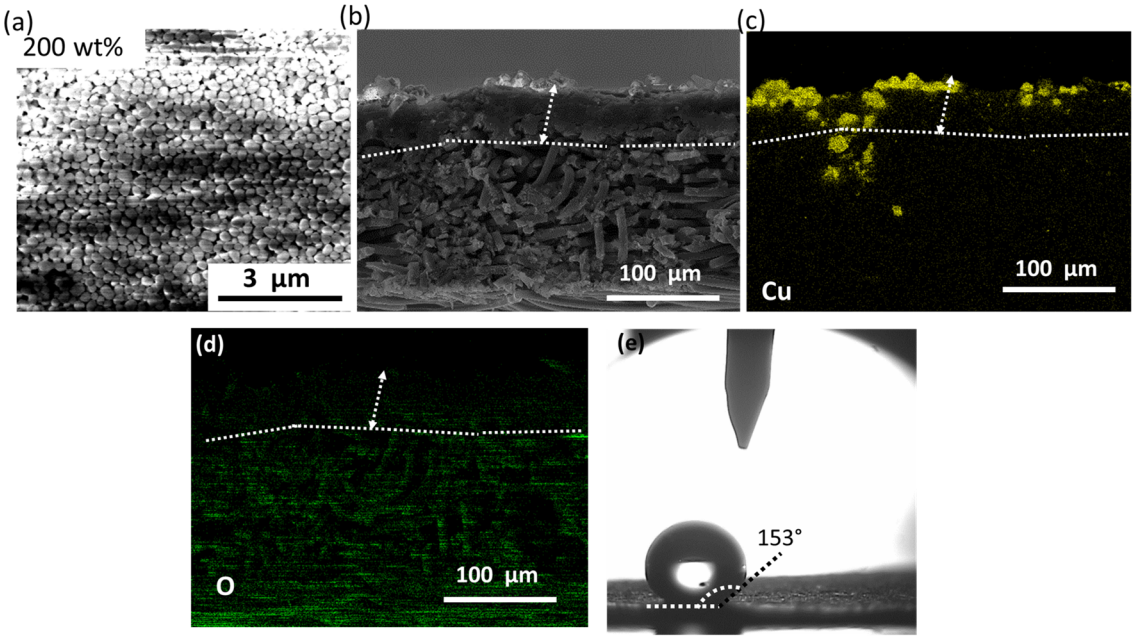

Figure S17: HKUST@800: (a) SEM images of 200 wt% PTFE supported GDE; (b) cross section view of the GDE; (c-d) SEM-EDS elemental color maps along the cross section showing the distributions of Cu and O; (e) contact angle value of the same GDE.

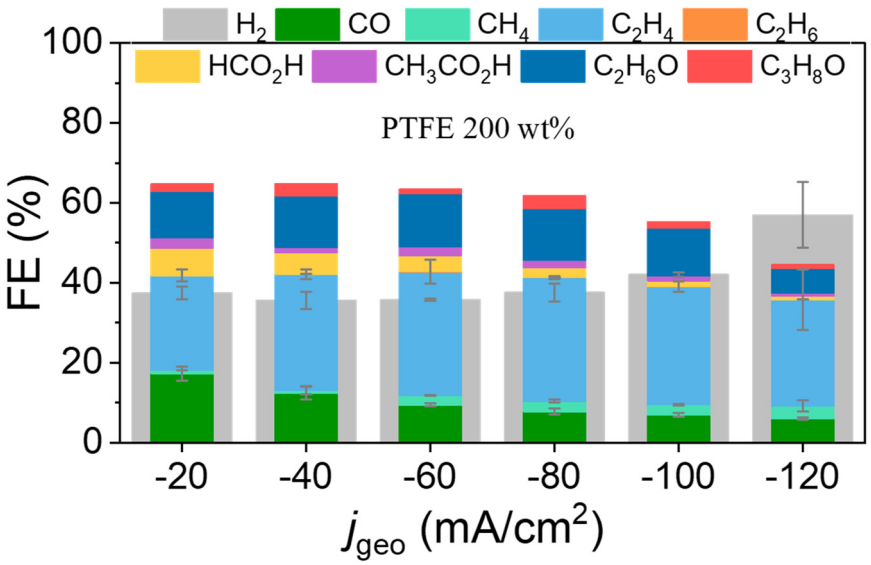

Figure S18: HKUST@800: %FE of the obtained products from the GDE containing 200 wt% PTFE loading at different current densities (j_{geo}) in 1 M KOH.

Post electrocatalysis analysis:

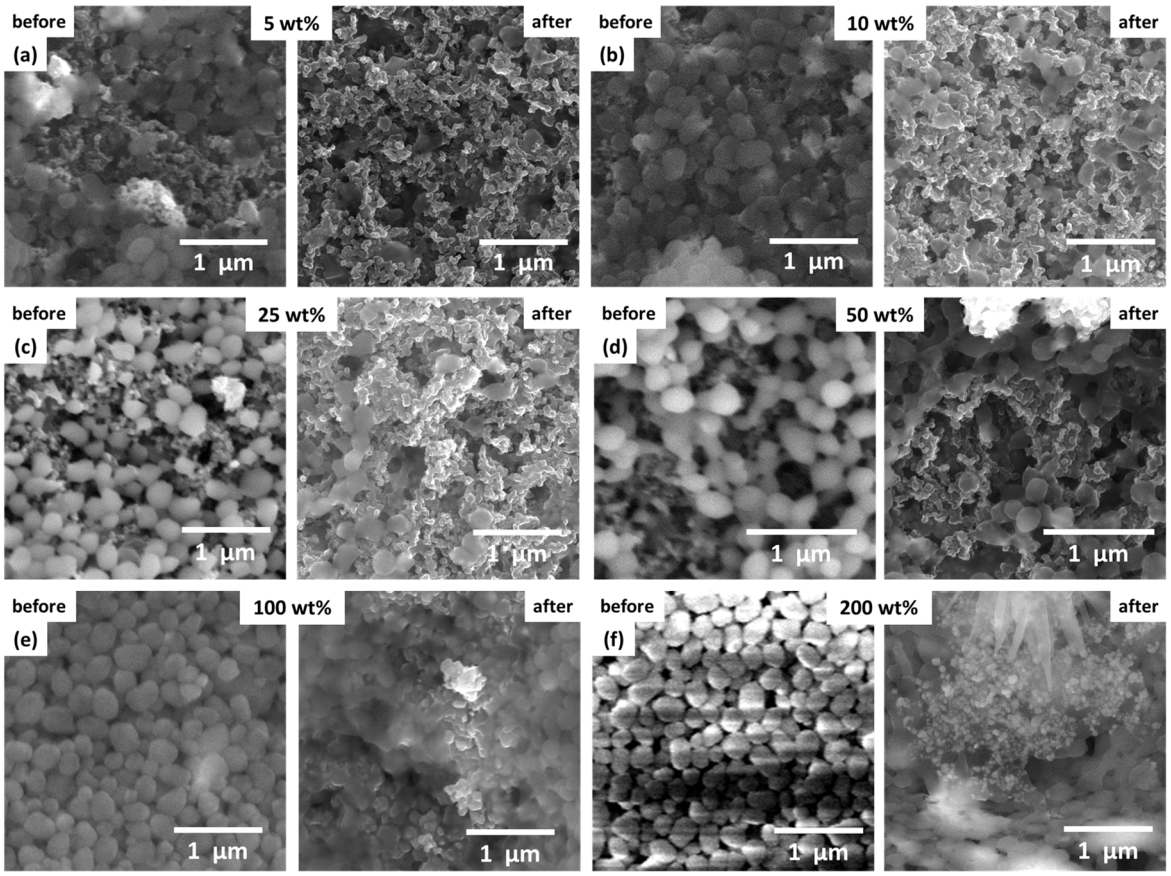

Figure S19: HKUST@800: SEM images of GDEs with different PTFE loadings, after performing electrocatalysis.

For TEM measurements a few representative electrodes were used e.g. 0, 10, 25, 50 and 100 wt% PTFE/HKUST@800 modified GDEs.

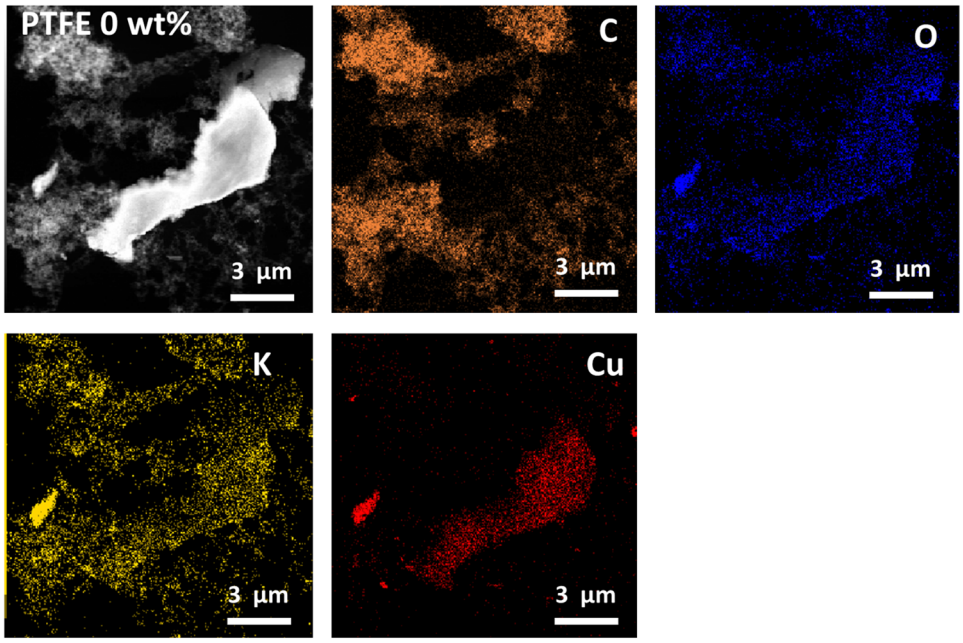

Figure S20: HKUST@800: TEM-EDS elemental color map images of 0 wt% PTFE modified GDE, showing irregular shaped catalyst particle agglomeration. Presence of potassium (K) indicates the formation of K_2CO_3/$KHCO_3$ during electrolysis.

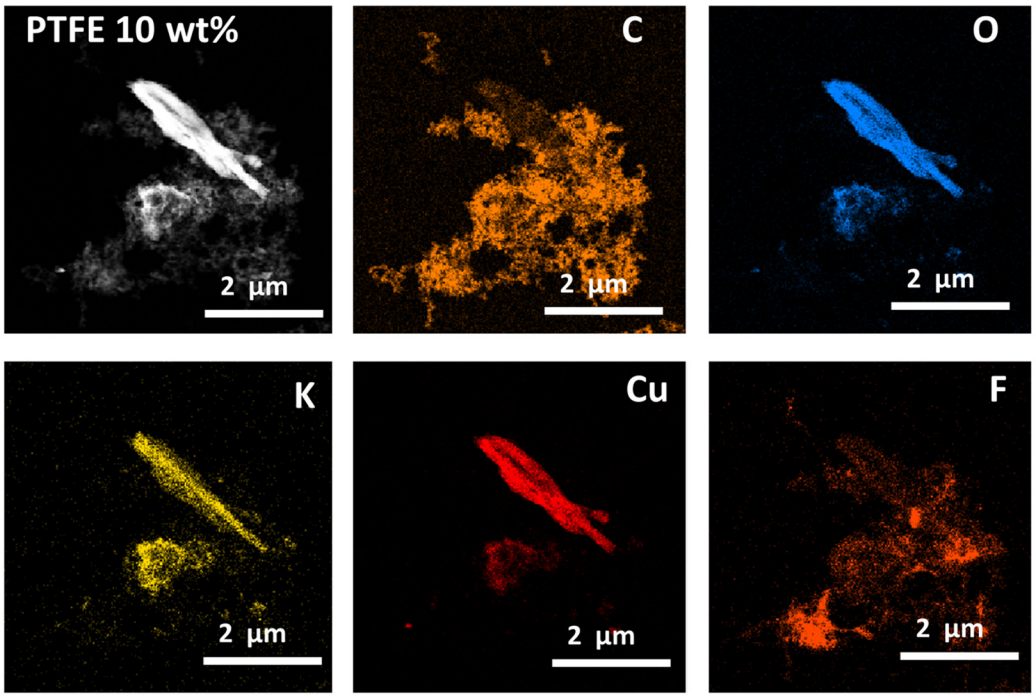

Figure S21: HKUST@800: TEM-EDS elemental color map images of 10 wt% PTFE modified GDE showing irregular shaped catalyst particle agglomeration. F represents PTFE.

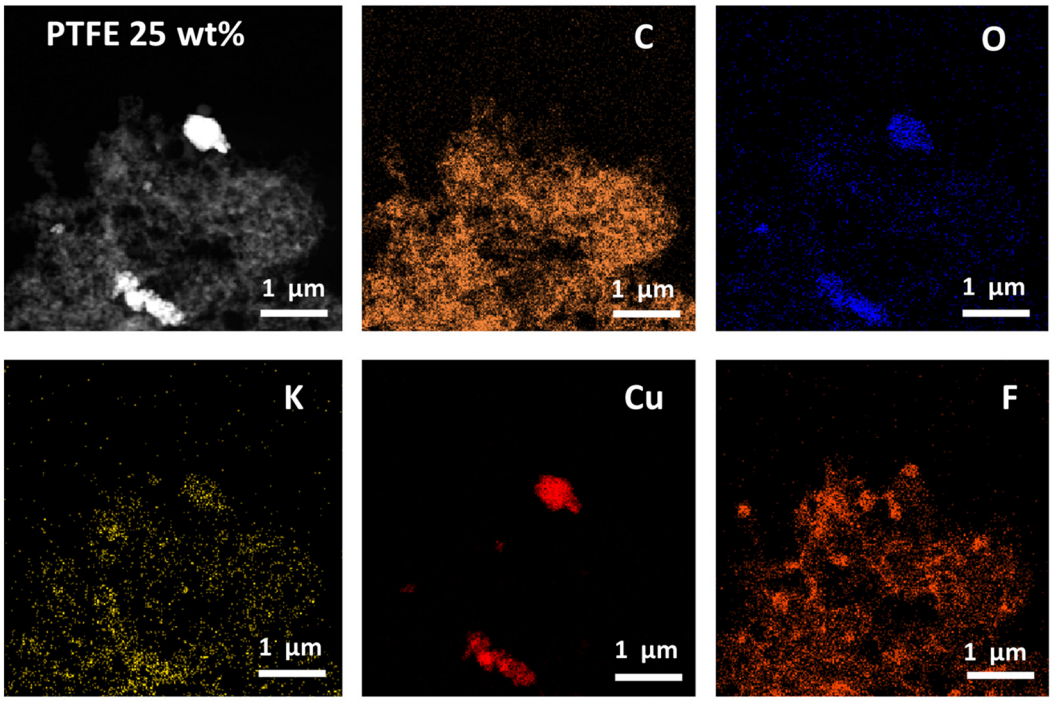

Figure S22: HKUST@800:TEM-EDS elemental color map images of 25 wt% PTFE modified GDE showing irregular shaped catalyst particle agglomeration. F represents PTFE.

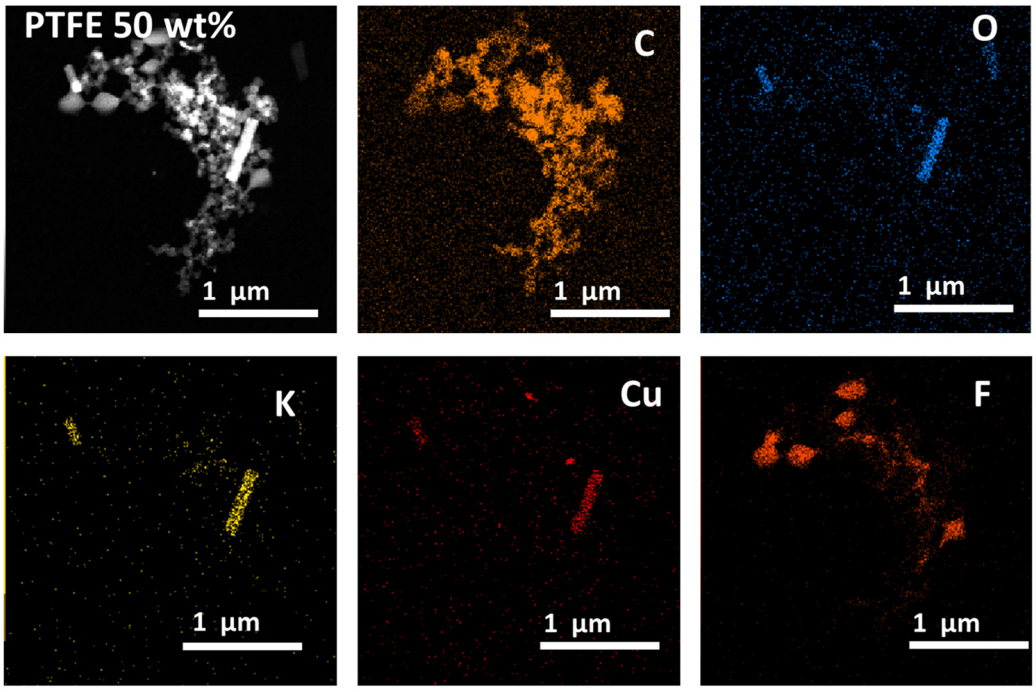

Figure S23: HKUST@800: TEM-EDS elemental color map images of 50 wt% PTFE modified GDE showing irregular shaped catalyst particle agglomeration. F represents PTFE.

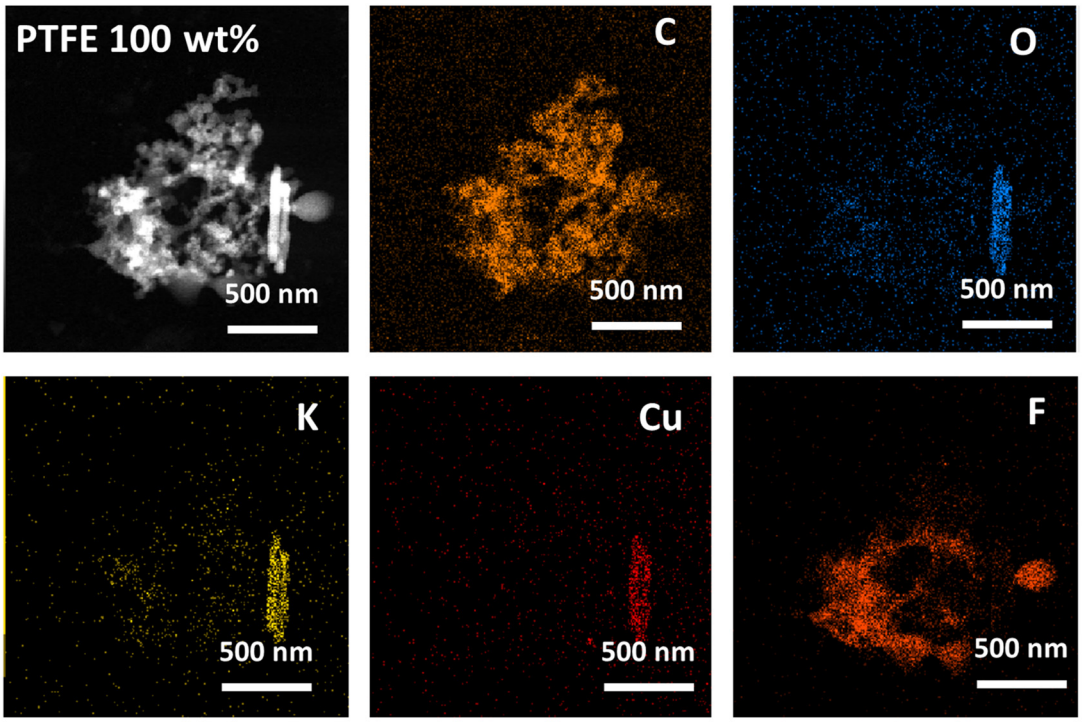

Figure S24: HKUST@800: TEM-EDS elemental color map images of 100 wt% PTFE modified GDE showing large irregular shaped catalyst particle agglomeration. F represents PTFE.

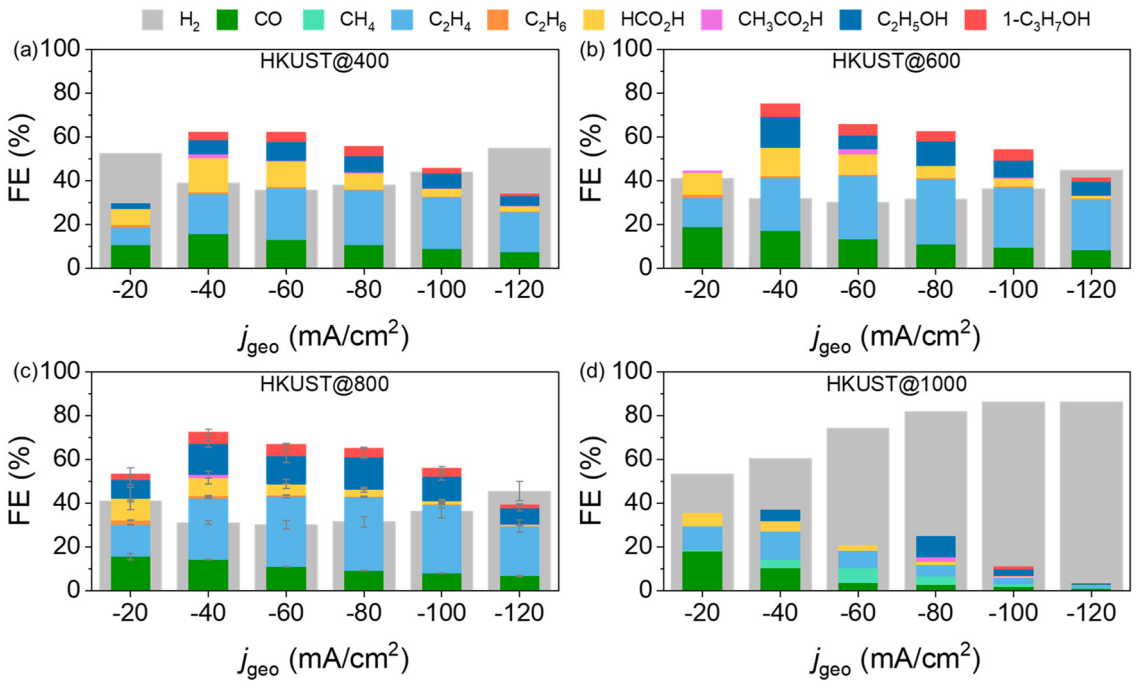

Figure S25: FE (%) for all products as obtained with HKUST@400, HKUST@600, HKUST@800 and HKUST@1000 mixed with 25 wt% PTFE on the GDEs at different applied current densities.

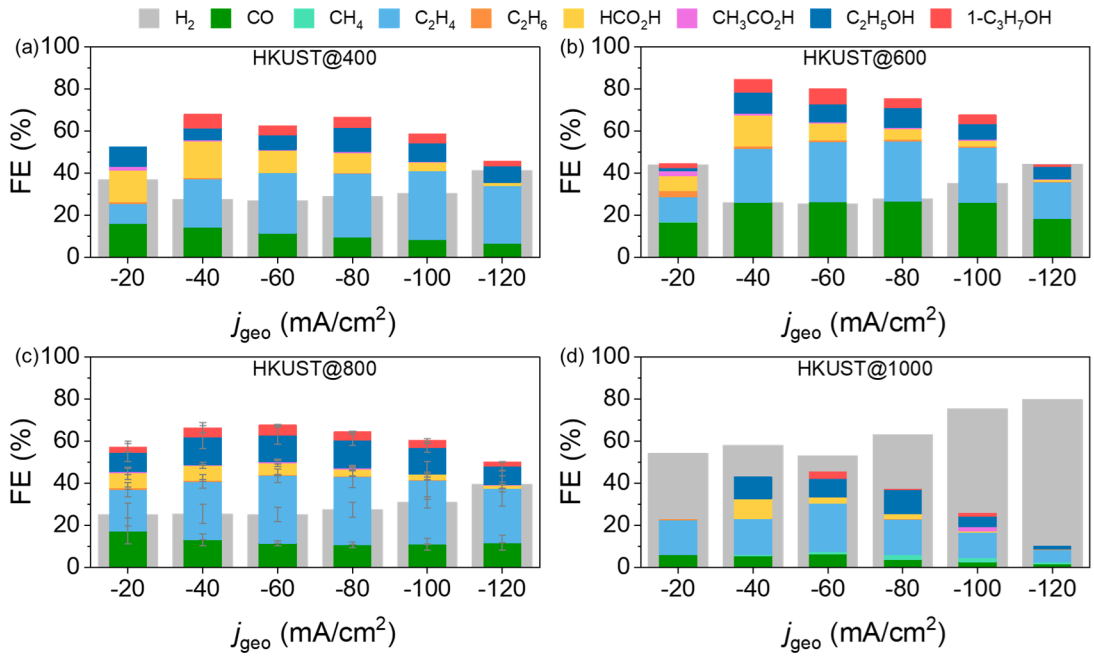

Figure S26: FE (%) for all products as obtained with HKUST@400, HKUST@600, HKUST@800 and HKUST@1000 mixed with 50 wt% PTFE on the GDEs at different applied current densities.

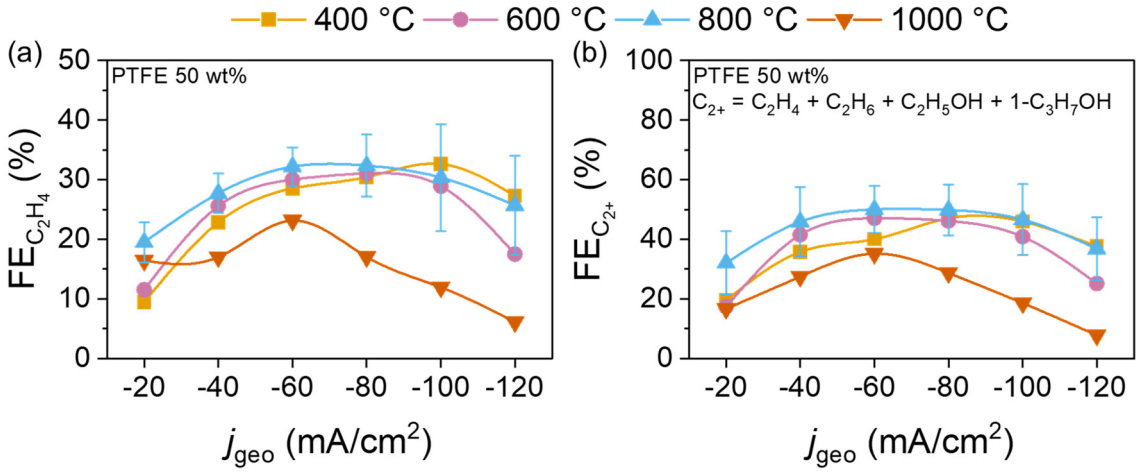

Figure S27: %FE_{C2H4} and %FE_{C2+} as obtained from HKUSTderived catalysts mixed with 50 wt% PTFE at different applied current densities.

Preparation of Pt-ultramicroelectrodes:

Pt-ultramicroelectrodes (UMEs) for the shear-force based SECM measurements were prepared using a laser puller (Sutter Instruments) following a previously published procedure[2] First, a Pt wire (Ø: 25 mm; Goodfellow) was positioned in the center of a quartz glass capillary ($Ø_{out}$: 0.9 mm, $Ø_{in}$: 0.3 mm, L: 90 mm; QSIL). After fixing the filled capillary in the laser puller unit and connecting both capillary inlets to a vacuum pump, the wire was sealed into the capillary within 7 – 12 heating/cooling cycles (20 s and 40 s Laser ON/OFF) using the following parameter set: Heat: 780; Filament: 5; Velocity: 150; Delay: 128, Pull: 0. Subsequent to the sealing step, the hard pull of the capillary was carried out with the following parameters: Heat: 775; Filament: 5; Velocity: 150; Delay: 128, Pull: 170. Pt-UMEs obtained from the laser pulling procedure were then electrically contacted by soldering a Cu wire (Ø 22 mm; BLOCK) to the non-sealed part of the Pt wire through short heating with a heat gun. Afterwards, Pt-UMEs were transferred into a dual-beam FIB/SEM instrument (Quanta 3D ESEM; FEI) in order to open the glass-covered tip by FIB milling. For that purpose, a Ga ion beam (15 nA

current and 30 kV acceleration voltage) was focused on the desired position of the Pt/glass body exposing a tip consisting of a disc shaped Pt-surface surrounded by glass. In between different measurements the as-obtained Pt-UME was stored in 2 M HNO_3 solution to avoid contamination.

Shear-force approach and measurement of local hydroxide/water activity:

Positioning of the Pt-UME close to the surface of a GDE was conducted by means of shear force distance-control scanning electrochemical microscopy (SECM). In this method, hydrodynamic forces in close proximity to a solid surface exert influence on the characteristics of an electrode´s oscillation making the methodology independent of electrochemical feedback mechanisms.[3] In order to establish a shear-force based distance control loop, two piezo elements (Piezomechanik Pickelmann) glued on top of brass holders were mounted directly to the UME's electrode body. The piezo element close to the tip's taper served as a detection element for the vibrational movements of the tip apex. 1 – 1.5 cm away from the detection piezo, the excitation piezo was mounted at an angle of around 45 °. Both piezo elements were connected to a lock-in amplifier (Ametek 7280). By applying different AC voltages to the excitation piezo, oscillations with defined frequencies were applied to the tip apex, while the detection piezo enabled the measurement of magnitude and phase of oscillation.

Prior to the positioning of the Pt-UME with the attached piezo elements, the GDE sample was mounted in a cell body made from PEEK (Figure S28) which was specifically designed for SECM experiments with UMEs positioned over GDEs. Two gaskets (Ø: 28 mm, *Viton*®) with an inner hole of 5 mm diameter sandwiched the GDE in order to confine CO_2 in the gas compartment at the GDE backside. An additional O-ring with an inner diameter of 5 mm pressed on the GDE side facing the electrolyte, thus confining the electrolyte to a geometric surface area of 0.2 cm^2. Prior to the experiment gas lines were purged > 30 min with CO_2. Pre-alignment of the Pt-UME to the GDE surface was controlled by help of a video microscope (monochrome USB camera; The ImagingSource) performing movements in x, y and z direction with stepper motors (OWIS). Determination of the Pt-UME's characteristic resonance frequency was accomplished by comparing frequency spectra (frequency range: 200 – 500 kHz, amplitude: 150 mV) recorded in air and in bulk solution after filling electrolyte (exemplary spectrum in Figure S29). The electrolyte level was adjusted to not be in contact with the detection piezo. Before the electrolyte was filled into the SECM cell, it was purged > 20 min with Ar to remove dissolved oxygen. Ar flow above the electrolyte was maintained to mitigate the re-dissolution of oxygen from the atmosphere.

Once resonant frequencies of the tips were identified, the most time-stable of those frequencies was set to the Pt-UME and the latter was incrementally approached towards the GDE surface using a piezo-based positioning system (PI, Germany). Throughout the approach, magnitude and phase of the tip's oscillation were recorded. A magnitude variation of 2 % of the lock-in value was used as a stop-criterion for the approach (exemplary approach curve in Figure S29). After positioning the Pt-UME in the shear-force interaction region of the GDE sample, a CO_2 flow of ~20 mL/min was adjusted in the gas channel behind the GDE backside through a mass flow controller (Model: GFC17, Aalborg). The CO_2 gas outlet tube was positioned in a water-filled glass column and placed < 1 cm below the water level in order to achieve an overpressure of 1 mbar within the CO_2 gas line.

Electrochemical measurements were recorded using a bi-potentiostat (IPS PG 100) controlled by an in-house programmed software. The GDE and the Pt-UME were connected as working electrode 1 and 2, respectively. After electrolyte was filled into the cell and the electric circuit was closed, a resting potential of -0.1 V vs. double junction Ag|AgCl (3 M KCl) reference electrode (100 wt% PTFE sample) and -0.5 V (0 wt% PTFE sample) was applied to the GDE resulting in a reductive current of a few µA. From that point on, cyclic voltammograms (200 mV/s, Start/Stop potential: 0 V) were continuously recorded at the Pt-UME adjusting the upper and lower vertex potentials to avoid excessive oxygen or hydrogen evolution reaction. Simultaneously, the GDE current and potential were measured. Starting from the initial resting potentials at the GDE, the potential was incrementally shifted to more negative potentials in order to attain currents of -4 mA, -8 mA, -12 mA, -16 mA, -20 mA and -24 mA at the GDE. The GDE current was stabilized at each increment by manual readjustment of the potential (pseudo-galvanostatic measurement principle). Only once the peak current recorded at the Pt-UME stabilized for each condition, the GDE current was incremented to the next value. After probing the highest

GDE current of -24 mA, the GDE was switched back to the initial resting potential while recording the time-development of the Pt-UME CVs until stabilization.

Calibration of the PtO-reduction peak potential was performed subsequently to the SECM experiment. KOH calibration solutions were prepared from a 16 M KOH (99.9 % Trace metal basis, semiconductor grade), whose titer factor was determined as 0.991 by titration with oxalic acid dihydrate (Merck) with phenolphthalein as indicator. Each calibration solution was filled into a polypropylene petri-dish. The Pt-UME, as well as the same counter and reference electrode compartment as in the SECM experiment, were positioned in the petri-dish. Cyclic voltammograms were recorded in each calibration solution (2 M, 4 M, 8 M, 12 M and 16 M) using similar vertices as in the SECM experiment.

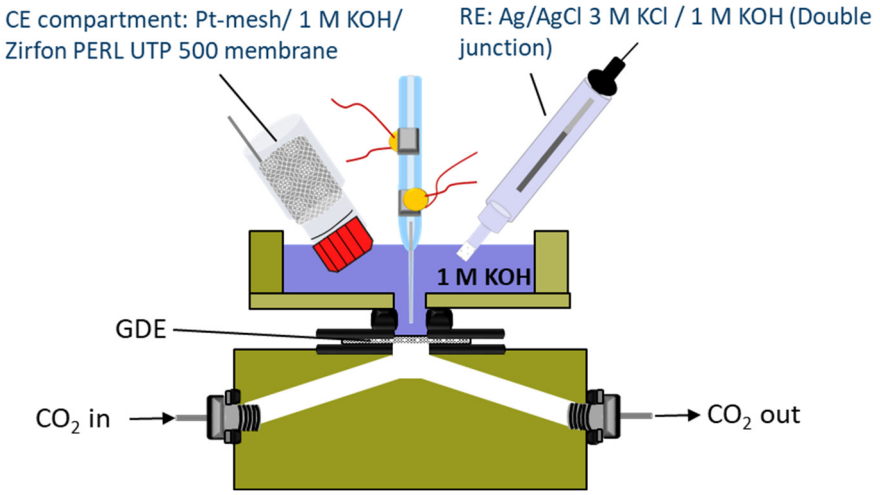

Scheme S2: Scheme of the GDE-SECM cell body made from PEEK which illustrates the Pt-UME, counter electrode and reference electrode positioning in the electrolyte compartment.

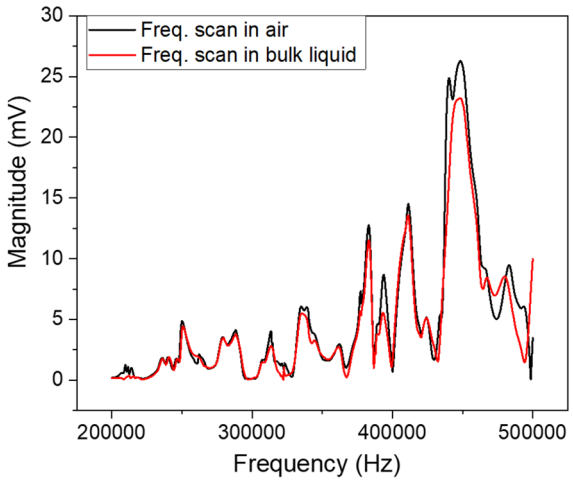

Figure S28: Frequency scans of the Pt-UME in air and bulk liquid.

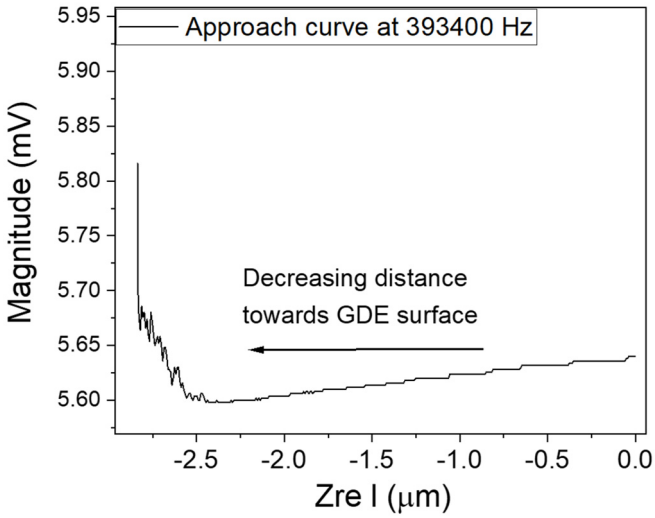

Figure S29: Representative plot of an approach curve obtained during approach of a Pt-UME to a HKUST@800 – 0 wt% PTFE GDE.

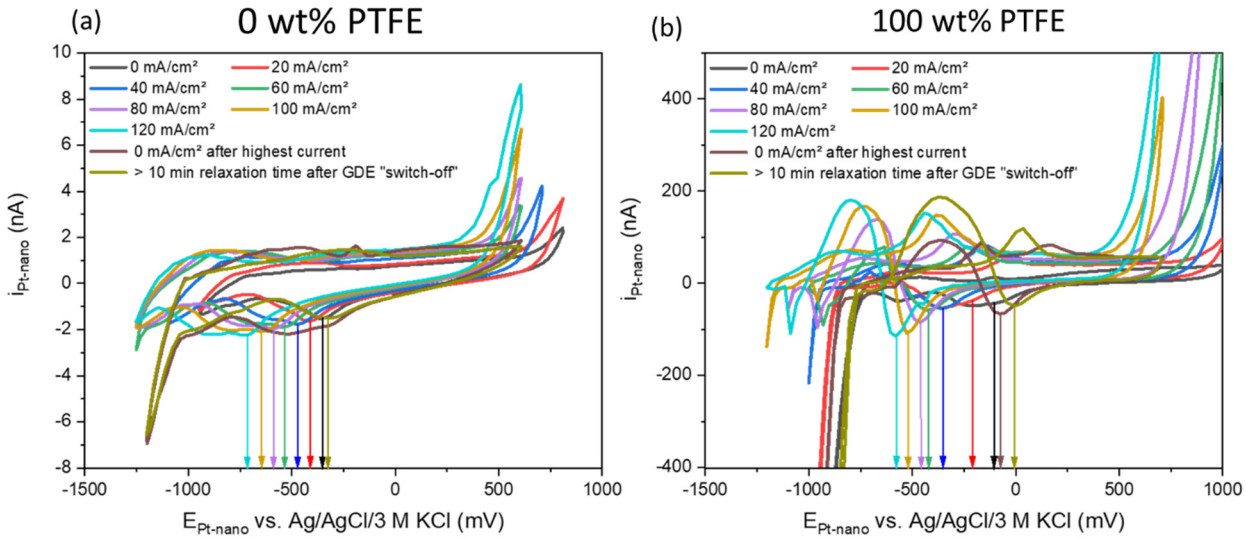

Figure S30: (a) Representative cyclic voltammograms of a Pt-UME approached to a HKUST@800 – 0 wt% PTFE modified GDE for different currents (b) representative cyclic voltammograms of a Pt-UME approached to a HKUST@800 – 100 wt% PTFE for different GDE currents.

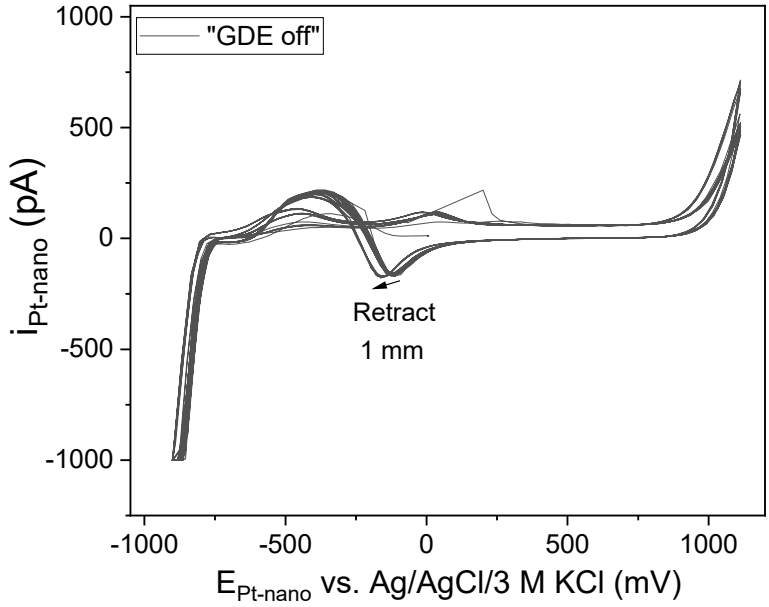

Figure S31: Cyclic voltammograms of a Pt-UME approached to a HKUST@800 – 100 wt% PTFE while the GDE was held at -100 mV vs. reference (named as “GDE off” state). During recording of the cyclic voltammograms the Pt-UME was 1 mm retracted from the GDE surface.

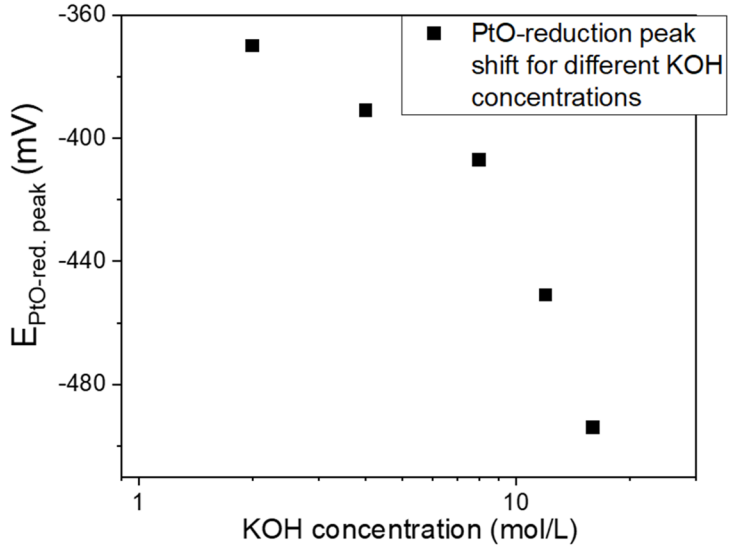

Figure S32: (a) Peak potential position of a Pt-UME immersed into calibration solutions of different KOH concentrations (b) cyclic voltammograms (200 mV/s) at a Pt-UME recorded in different KOH calibration solutions outside the SECM cell in a petri-dish.

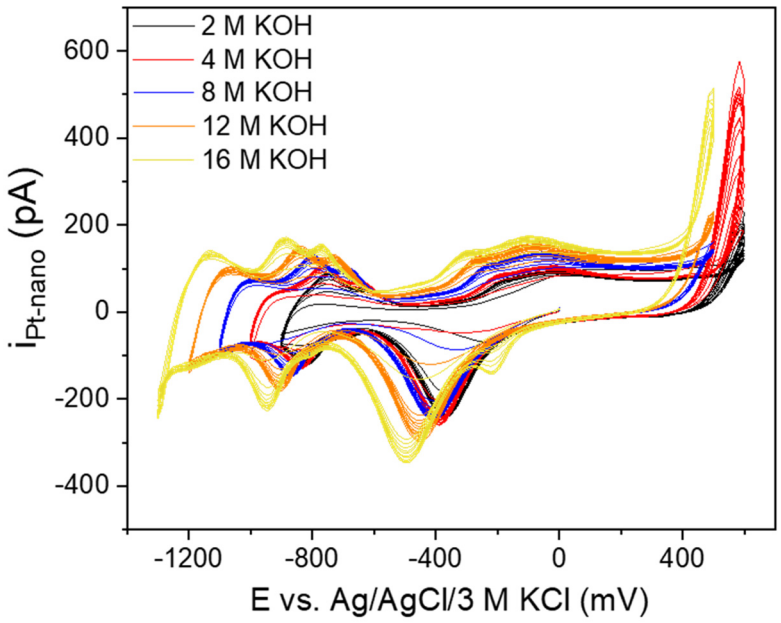

Figure S33: Cyclic voltammograms (200 mV/s) at a Pt-UME recorded in different KOH calibration solutions outside the SECM cell in a petri-dish.

[1] a) X-ray Photoelectron Spectroscopy (XPS) Reference Pages: Copper (xpsfitting.com), b) M.C. Biesinger, *Surf. Interface Anal.* **2017**, *49*, 1325-1334, c) M.C. Biesinger, L.W.M. Lau, A.R. Gerson, R.St.C. Smart, *Appl. Surf. Sci.* **2010**, 257, 887-898

[2] B. B. Katemann, W. Schuhmann, *Electroanal.* **2002**, *1*, 22.

[3] a) R. Brunner, A. Bietsch, O. Hollricher, O. Marti, *Rev. Sci. Instrum.* **1997**, *68*, 1769; b) M. Ludwig, C. Kranz, W. Schuhmann, H. E. Gaub, *Rev. Sci. Instrum.* **1995**, *66*, 2857.